Supporting information

Carbon nanofibers bridged two-dimensional titanium carbide as a superior anode in lithium-ion battery

Zongyuan Lin,[a] Dongfei Sun,[a] Qing Huang*[b], Jun Yang,[a]

Michel W. Barsoum,[c] and Xingbin Yan*[a]

[a] Laboratory of Clean Energy Chemistry and Materials, State Key Laboratory of Solid Lubrication, Lanzhou Institute of Chemical Physics, Chinese of Academy of Sciences, Lanzhou, 730000, China

E-mail: xbyan@licp.cas.cn

[b] Division of Functional Materials and Nano-Devices, Ningbo Institute of Material Technology and Engineering, Chinese Academy of Science, Ningbo, 315201, China

E-mail: huangqing@nimte.ac.cn

[c] Department of Materials Science and Engineering, and A. J. Drexel Nanomaterials Institute, Drexel University, Philadelphia, PA 19104, United States

Experimental

Synthesis of multilayer $Ti_3C_2T_x$ particles: The Ti_3AlC_2 MAX phase was prepared according to the reported method.[1] Multilayer $Ti_3C_2T_x$ particles were prepared by exfoliating the Al element from the Ti_3AlC_2 in 40 % HF solution at room temperature for 24 h. The mixture was then centrifuged and the resulting powder was thoroughly washed using deionized, DI, water, and then dried by lyophilization.
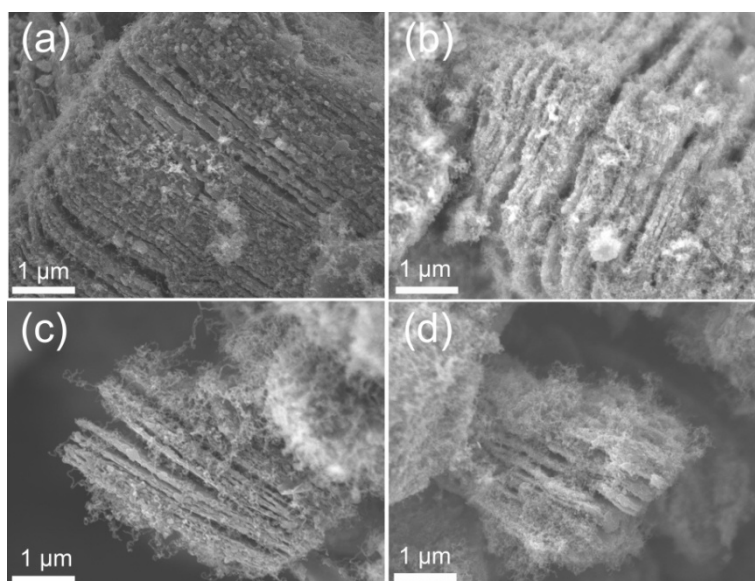
Synthesis of Ti_3C_2/CNF hybrid particles: Ti_3C_2/CNF hybrid particles were prepared by a simple nanocasting followed by a chemical vapor deposition for growing CNFs. In a typical process, 20 mg of poly(vinyl pyrrolidone) (PVP, Mw=1,300,000) and 200 mg of $Co(NO_3)_2 \cdot 6H_2O$ were dissolved in 16 ml of DI water to form a solution containing the catalyst precursor. As-prepared multilayer $Ti_3C_2T_x$ particles were placed in a Schlenk flask and a vacuum was applied using a vacuum pump. The above solution was added into the flask for it to vacuum impregnate the MXene flakes, before sonication for 30 min. The resulting suspension was centrifuged to remove the supernatant and the impregnated $Ti_3C_2T_x$ particles were dried at 60 °C in air. For comparison, $Co(NO_3)_2 \cdot 6H_2O$ with different masses (40, 100, 300 and 400 mg) were used, respectively.

The dried $Ti_3C_2T_x$ particles containing PVP and the Co salt were placed in a horizontal quartz tube furnace, heated to 600 °C under an Ar (180 sccm)/H_2 (20 sccm) atmosphere, and then acetylene was introduced as the carbonaceous source for 0.5 h with a flow rate of 10 sccm. After rapid cooling to room temperature, the as-obtained black powders were treated with a 37 wt.% hydrochloric acid to remove Co catalyst, washed by DI water, and then dried by lyophilization.

Structural characterization: The morphology and microstructure of the samples were characterized by a field emission scanning electron microscope (FE-SEM, JSM 6701F) and a transmission electron microscope (TEM, JEOL 2100 FEG). X-ray photoelectron spectroscope (XPS, Physical Electronics, PerkinElmer PHI-5702) was employed to examine the surface chemical species of $Ti_3C_2T_x$ after the high-temperature at 600 °C. The XRD patterns were recorded by a powder diffractometer (PANalytical X'Pert PRO) with Cu Kα radiation (λ= 1.5418 Å). The specific surface area and pore structure of samples were measured and analyzed using a Micromeritics ASAP 2020 volumetric adsorption analyzer and Brunauer-Emmettp-Teller (BET) method. The contents of carbon in samples were analyzed by Elemental Analyzer (Vario EL).

Preparation of Li-ion cell: Each working electrode was prepared by mixing 80 wt.% anode active material, 10 wt.% acetylene black and 10 wt.% polyvinylidene fluoride with the aid of N-methy pyrrolidinon. The mixture was spread on a Cu foil and dried at 105 °C for 12 h under vacuum. After been pressed, the electrode (about 10 μm thick) was assembled into a coin cell (CR2032) in an argon-filled glove box using 1 M $LiPF_6$ in ethylenecarbonate (EC) and diethylenecarbonate (DEC) (1:1 volume ratio) as the electrolyte and Li metal as the counter electrode.

Electrochemical measurements: The capacity and cycling tests of coin cells were measured using a CT2001A cell test instrument (LAND Electronic Co.) in the voltage range of 0.01-3 V (vs. Li/Li$^+$). CV curves and EIS plots were recorded using an electrochemical workstation (CHI660D, Shanghai, China). The specific capacity was calculated based on the weight of active material. In our experiments, we built and tested more than three cells for each sample, and the capacity value for each sample shown in the paper was the average value.
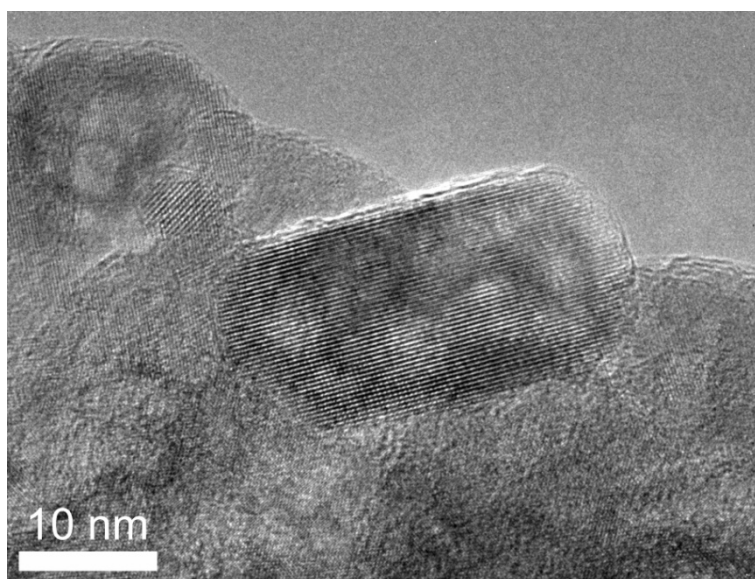
Figure S1. SEM images of Ti$_3$C$_2$-CNF hybrid particles prepared with different Co catalyst concentrations: Ti$_3$C$_2$-CNF-1-2 (a), Ti$_3$C$_2$-CNF-1-5 (b), Ti$_3$C$_2$-CNF-1-15 (c), and Ti$_3$C$_2$-CNF-1-20 (d).
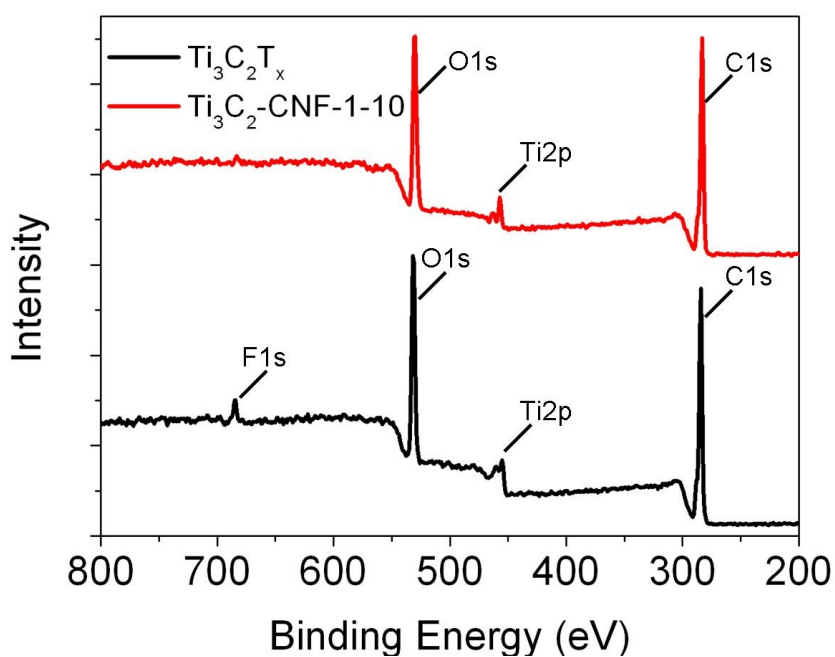
Figure S2. XPS spectra of pure Ti$_3$C$_2$T$_x$ particles before and after the heat-treatment at 600 °C under Ar/H$_2$ atmosphere.

There was no obvious F signal in the XPS spectrum of Ti$_3$C$_2$T$_x$ particles after the heat-treatment, indicating the removal of the surface F atoms. Moreover, because lamelleted materials are easy to absorb water, Fourier transform infrared spectrometer

(FTIR) cannot be employed to examine the surface -OH species. But, as shown in XRD pattern of $Ti_3C_2T_x$ particles after the heat-treatment (Figure S4), the formation of TiO_2 indicated the partial oxidation of Ti in Ti_3C_2 because of the existence of oxygen originating from oxygen-containing groups. It also indicated the disappearance of –OH groups after the heat-treatment.


**Figure S3.** TEM image of anatase TiO_2 nanoparticles formed on the surface of Ti_3C_2 phase.
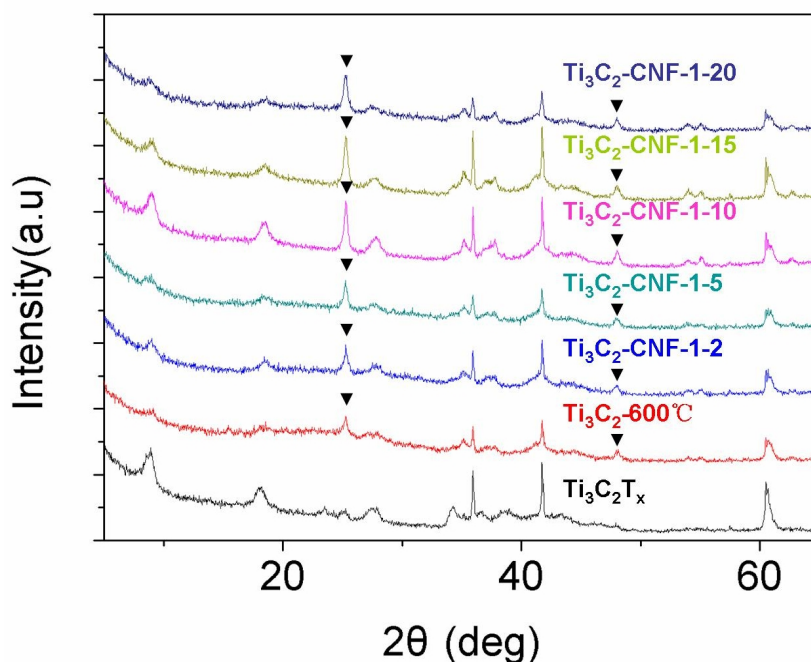
Figure S4. XRD patterns of Ti_3C_2-CNF hybrid particles prepared with different Co catalyst concentrations. For comparison, the XRD patterns of pure $Ti_3C_2T_x$ particles before and after the heat-treatment at 600 ℃ were measured and listed as well. The peaks attributed to anatase have been marked by inverted triangle.
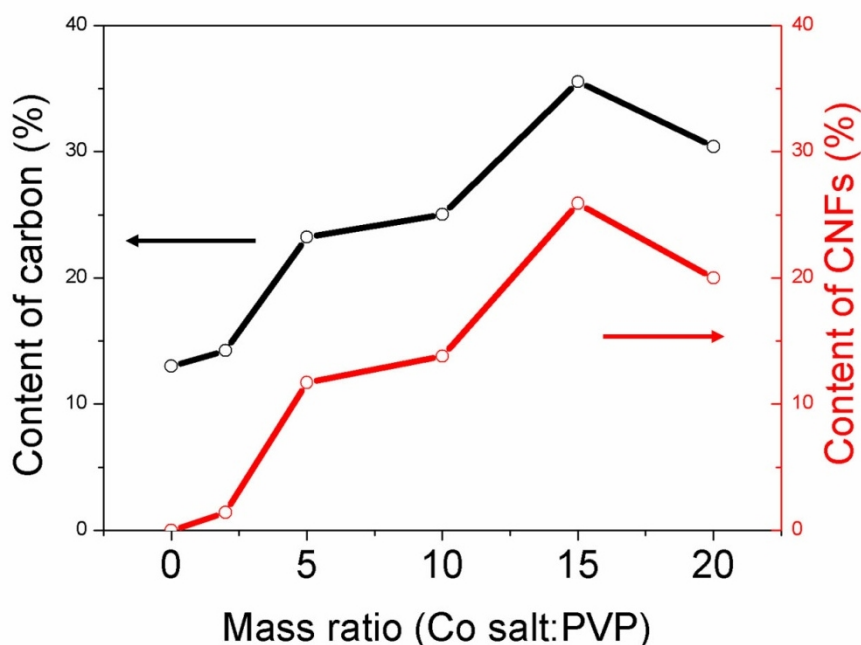
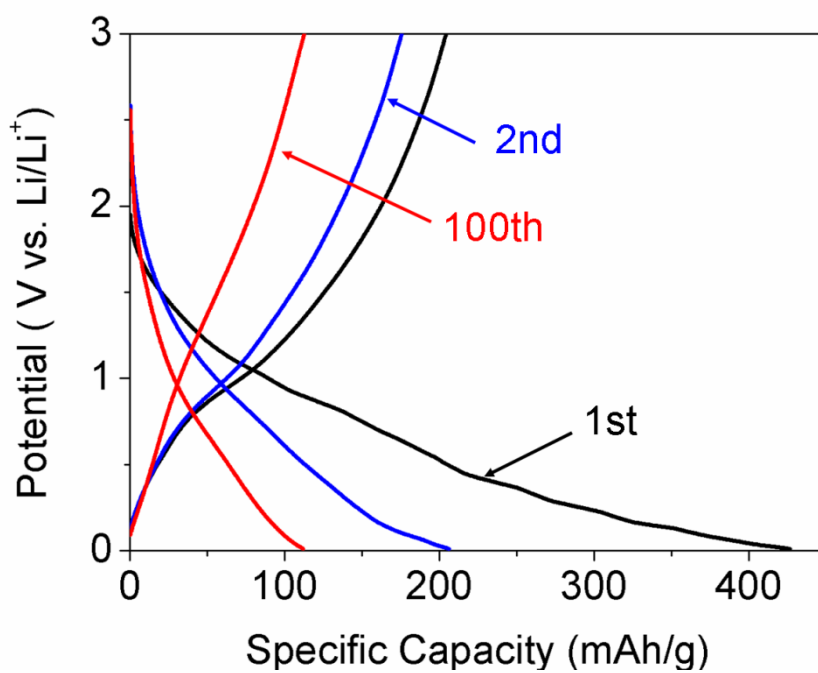**Figure S5.** Total carbon content and CNF content in the Ti_3C_2/CNF hybrid samples as a function of the mass ratio (Co salt to PVP) in preparation of the samples.
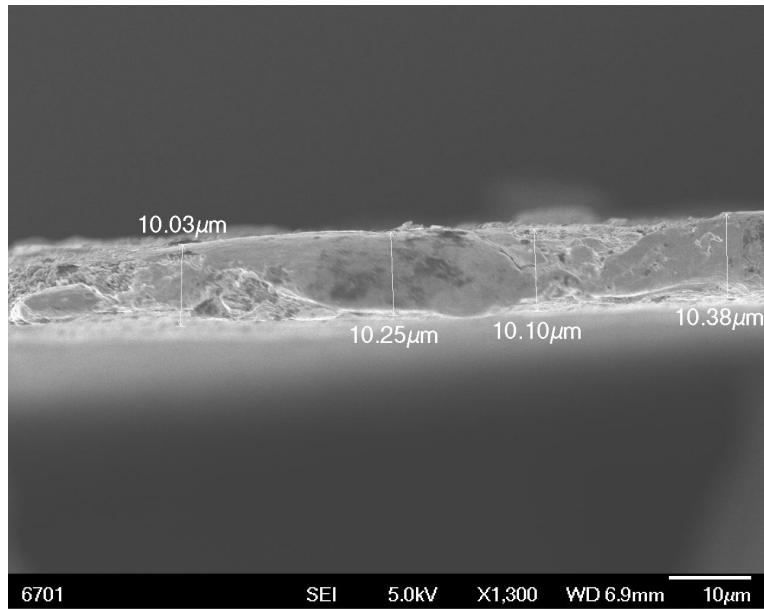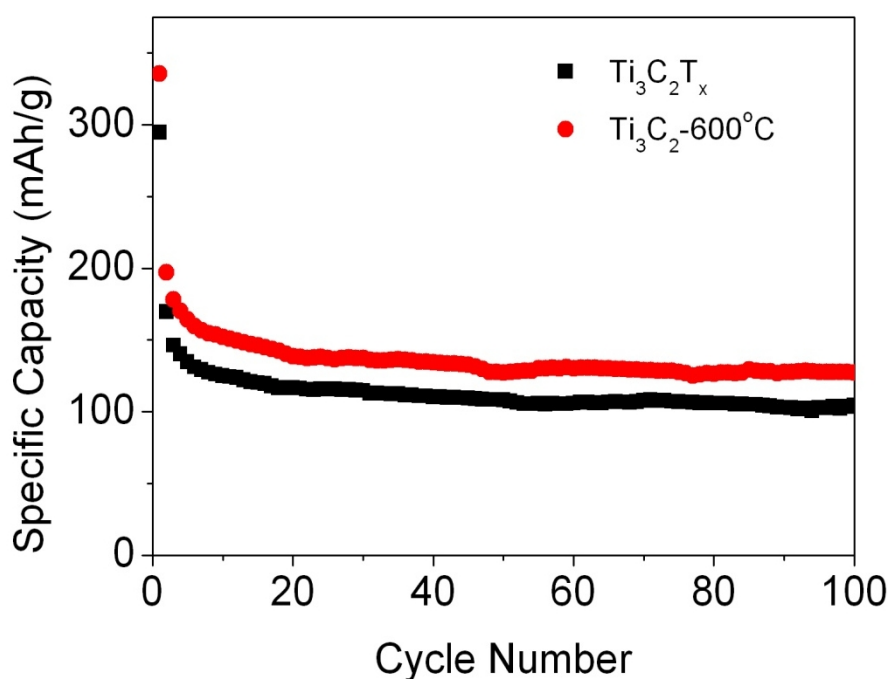
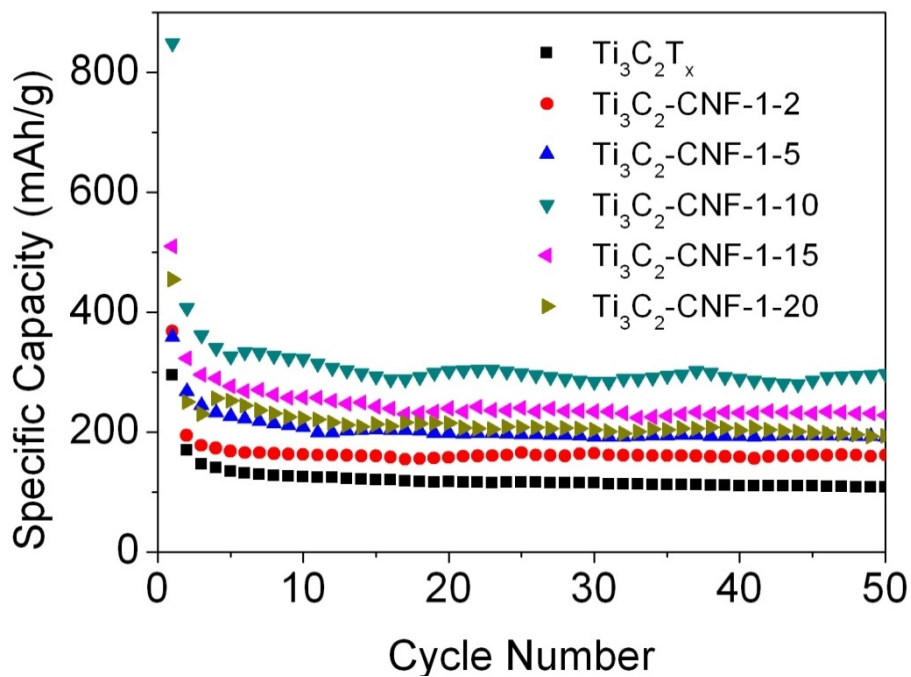**Figure S6.** Cross-section SEM image of a working electrode.
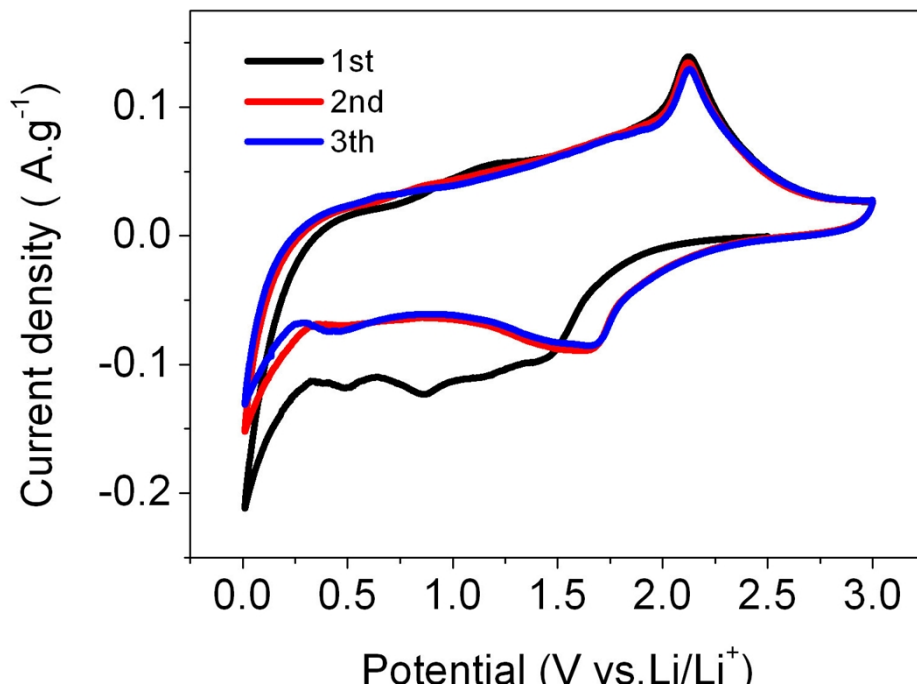
Figure S7. The CV curves of Ti$_3$C$_2$-CNF-1-10 sample at the sweep rate of 0.2 mV/s.
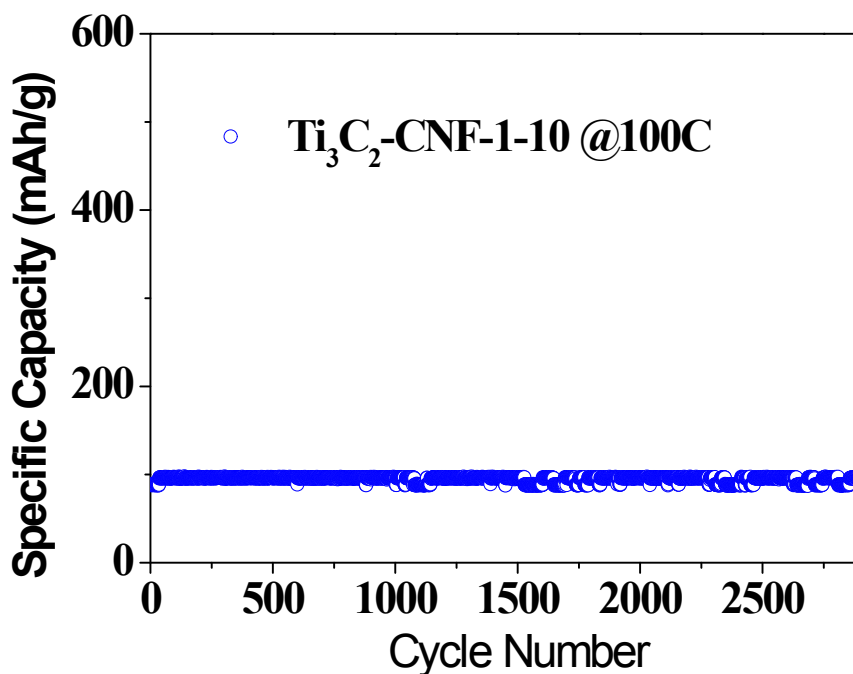
Figure S8. The charging/discharging curves of pure $Ti_3C_2T_x$ sample at 1 C.

Figure S9. The capacities of pure $Ti_3C_2T_x$ particles before and after the heat-treatment at 600 °C under Ar/H_2 atmosphere at the same current density of 0.32 A g^{-1}.
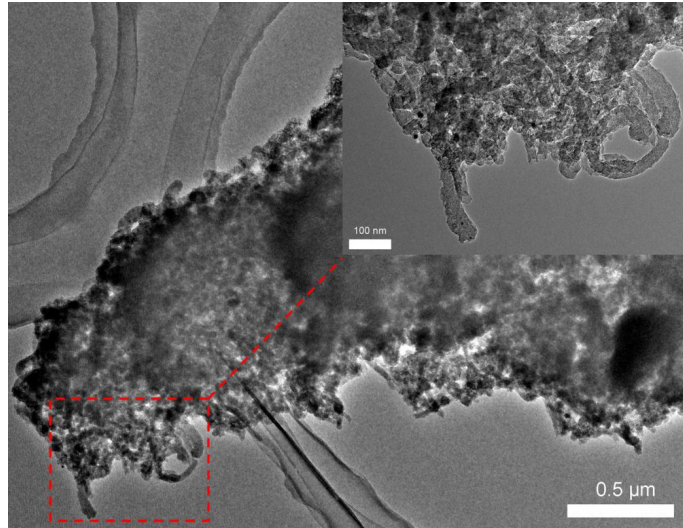
Figure S10. Specific capacities as a function of CNF content. The current density

for all electrodes was 0.32 Ag^{-1}.

Figure S11. The cycling stability of Ti$_3$C$_2$-CNF-1-10 sample at 100 C for 2900

cycles.

Figure S12. TEM images of Ti$_3$C$_2$-CNF-1-10 sample after 2900 cycles.